Fluctuation effects in an epidemic model

C. P. Warren,[1] G. Mikus,[1] E. Somfai,[2] and L. M. Sander[1]
[1]*Michigan Center for Theoretical Physics, Department of Physics, The University of Michigan, Ann Arbor, Michigan 48109-1120*
[2]*Instituut Lorentz, Leiden, NL-2333 CA, Netherlands*
(Received 14 December 2000; published 11 April 2001)

We study a discrete epidemic model $A+B\rightarrow 2A$ in one and two dimensions (1D and 2D). In 1D for low concentration θ, we find that a depletion zone exists ahead of the front and the average velocity of the front approaches $v=\theta/2$. In the 1D high concentration limit, we find that the velocity approaches $v=1-e^{-\theta/2}$. In 2D, for low concentration we also find a depletion zone, and the velocity scales as $v\sim\theta^{0.6}$, which is different from the scaling expected from the mean field approximation, $v\sim\theta^{0.5}$. Analysis of the interface width scaling properties demonstrated that the front dynamics of this reaction are not governed by the Kardar-Parisi-Zhang equation.

DOI: 10.1103/PhysRevE.63.056103 PACS number(s): 05.40.−a, 82.20.−w, 82.65.+r

I. INTRODUCTION

In this paper we analyze a simple discrete model of the reaction $A+B\rightarrow 2A$ in one and two dimensions. We can think of this as a model for an epidemic: the A particles are sick, and they infect B's on contact. We are particularly interested in the spatial dynamics of the model, i.e., the velocity of propagation of the infection and the characteristics of the region around the moving front.

To be specific, we allow the particles to diffuse, i.e., perform a random walk on a lattice, and when a ''sick'' particle encounters a ''healthy'' one (a B particle) then the B is instantly infected. We assume that the A's and the B's affect see each other only by infection. Otherwise they are independent random walkers that do not interact. In one dimension (1d), if we start with one A on the extreme left of the system, we are asking for the time dependence of the location of the front, the rightmost A. In 2D, we are asking for the time dependence of the location of the rightmost A in each row, averaged over rows. There is some resemblance between this model and what happens in a real epidemic caused by agents that do not move long distances. $A+B\rightarrow 2A$ may also be thought of as an irreversible autocatalytic chemical reaction.

Models of this type have evoked a good deal of interest [1–5] because of several unexpected, fascinating features of the process. As we will see, in the limit of small θ the front propagation is dominated by fluctuation effects. What attracted particular attention [1] was the realization that, as a result, continuum modeling breaks down completely for this reaction.

To see this we note that we expect the mean concentration of A particles to be described by the Fisher-Kolmogorov (FK)equation [6].We start by writing a conventional reaction-diffusion equation:

$$\partial_t a = D\Delta a + kab = D\Delta a + ka(\theta - a). \tag{1}$$

Here k is a rate constant, D the diffusion constant, and in the second line we have used the fact that on average $a+b=\theta$. In one dimension, the last equation becomes the FK equation $\partial_t u=\partial_{xx}u+u(1-u)$ after changing variables. From the standard theory [7], the velocity of the front approaches $v_c=2\sqrt{kD\theta}$ independent of initial conditions. The key element in this sort of ''pulled front'' equation is that the velocity is determined by the exponential growth of a far ahead of the front where a is very small.

However, simulations [1] showed that in 1D the front velocity was *linear* in θ for small θ, and thus very much smaller than expected. This is partially understandable from the work of Brunet and Derrida [3], who pointed out that discreteness has an anomalously large effect on systems which obey the FK equation in the continuum limit. The FK equation is structurally unstable, sensitive to small perturbations. In Refs. [3,4] models were introduced that interpolate between the results of [1] and the FK equation via a very slow crossover. The models involve a very large density of particles with a small reaction rate. These authors found that the velocity depression was given by $v\sim v_c-K/\ln^2(\theta)$ where K is a constant. However, we find here that for our version of the model (large reaction rates, small density) fluctuations are the dominant effect. In both cases, the essential point is that the front dynamics are very easily perturbed by small effects since the velocity is determined in regions where a is tiny.

In this work we enquire about the mechanism for the small velocity for $\theta\rightarrow 0$ in the original (discrete) $A+B\rightarrow 2A$ process. In a trivial model of independent random walkers, it is startling that there is any interesting dynamics. The total density at any point is clearly given by a Poisson distribution. It turns out, however, that the front is not a typical point, and this is the key to the unexpected behavior.

We find that the small velocity is a giant fluctuation effect that is qualitatively as follows. Suppose we assume that the velocity is a monotonically increasing function of θ, and recall that for small θ there are large fluctuations in the local density. The front will move quickly through high density regions, and get stuck in the low density ones. Thus, on average, the motion will be dominated by configurations where the front is behind a gap in the distribution of B's. The front motion will be random, and not advance, as long as the rightmost A cannot convert a B. Our simulations and analysis support this picture.

In Sec. II, we present the 1D model and specifically look at the limits of small and large θ. Our analysis for small θ is

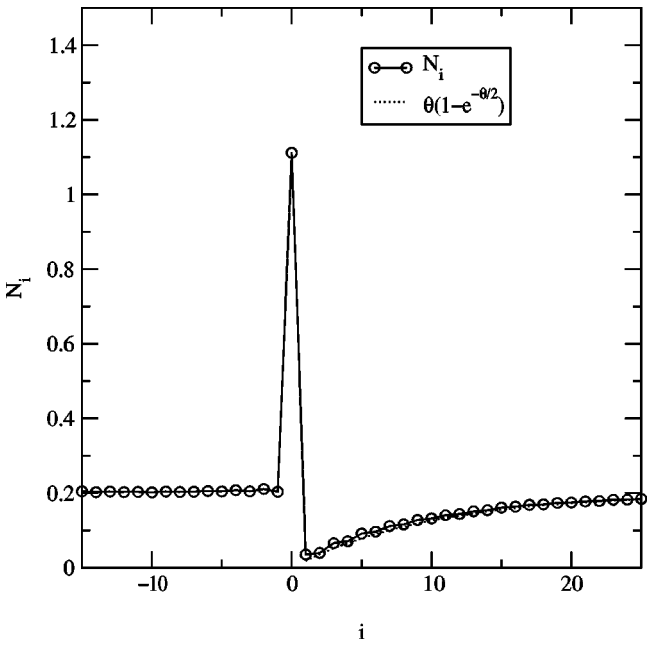

FIG. 1. Mean number of particles for sites near the front from a simulation with an average of 0.2 particles/site (in the rest frame of the front).

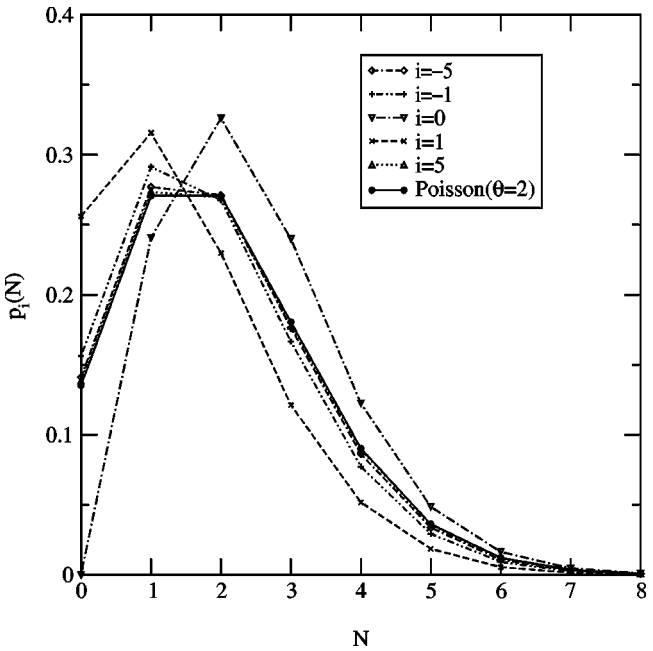

FIG. 2. Probability density of site *i* near the front from a simulation with an average of two particles/site (in the rest frame of the front).

more complete while our analysis for large θ consists of seeing to what extent we can use a Poisson approximation. In Sec. III, we present a two-dimensional version of the model with a view to seeing how much of this anomalous fluctuation effect carries over. We also analyze the interface width and see whether a scaling hypothesis holds, i.e., whether the front is self-affine.

II. THE 1D MODEL AND SIMULATION RESULTS

Consider a 1D lattice of length L [8] populated with random walkers randomly distributed with concentration θ [9]. The leftmost particle is of type *A*, and all of the other particles are of type *B*. The particles make random steps with parallel updating, i.e., all the particles move simultaneously. Any number of particles are allowed to occupy a site. If a *B* particle encounters or passes an *A* particle, it becomes an *A* particle. The rightmost *A* particle defines the propagation front, and we are interested in the velocity of this front.

The particles follow a simple random walk and thus are Poisson distributed. However, taking into account particle types and following the front, the particles near the front are not so distributed. Figure 1 shows the average density of particles from simulations for various sites around the front for $\theta=0.2$. Ignoring the fit for the moment, the density (conditioned on there being a front at $i=0$), is depleted to the right of the front. At higher concentrations, Fig. 2 shows the probability distribution of particles at various sites around the front in a simulation with average concentration $\theta=2$; Fig. 3 is for $\theta=8$.

Our simulations were performed in two different ways. For concentrations below $\theta=0.5$, 200 walkers were launched and $L=200/\theta$. Enough time steps were performed for each walker to walk on average halfway across the sample, $T=L/\theta$. To avoid initial transients calculations were also made with the first $40/\theta^2$ time steps censored. For concentrations above $\theta=0.5$, we used a 500-site lattice with 500θ walkers for 400 time steps, and the first 100 time steps were censored.

An earlier study [1] analyzed the velocity in an approximate fashion, using the Smoluchowski approach. In this method, centered in the rest frame of the front, *B* particles diffuse toward the front. The number density *n* follows the

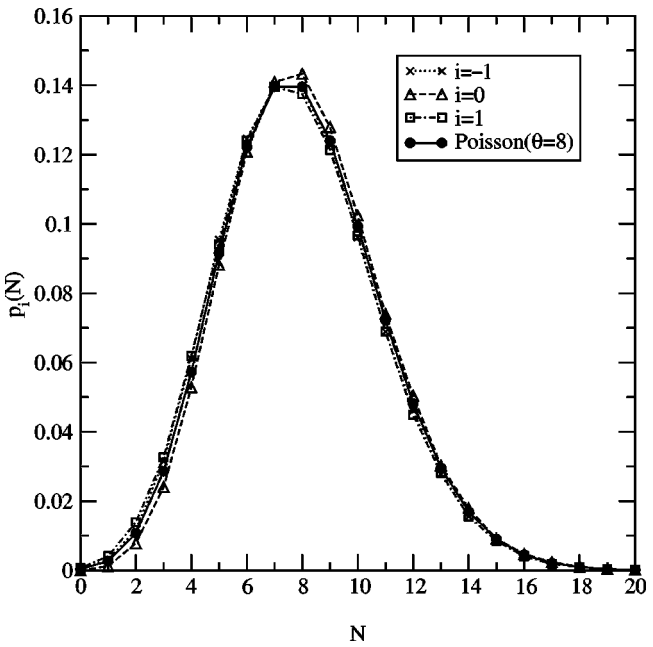

FIG. 3. Probability density of site *i* near the front from a simulation with an average of eight particles/site.

one-dimensional diffusion equation in the frame moving with velocity v,

$$\frac{\partial n}{\partial t} - v n' = n'', \tag{2}$$

where the diffusion constant $D=1$. Assuming stationarity, the time derivative vanishes, and the boundary conditions $n(\pm\infty)=\theta$, $n'(\pm\infty)=0$, and $n(0^+)=0$ lead to

$$n(x)=\begin{cases}\theta & \text{if } x<0\\ (1-\exp^{-vx})\theta & \text{if } x\geqslant 0.\end{cases} \tag{3}$$

We will see later that $v\propto\theta$ so that, as $x\to 0^+$, n is of order θ^2. As shown by Fig. 1, this distribution agrees well with the simulation. However, this analysis does not determine v.

A. Master equation for small θ

We are able to give an exact analysis in the low concentration limit, $\theta\ll 1$ Consider a region containing the front particle and the ''second'' particle, i.e., that nearest the front. (In the case of more than one particle at $i=0$ we arbitrarily declare one to be the front and the other the second particle.) The size of the region will be $\sim 1/\theta$. Define a coordinate system in the rest frame of the front particle, whose position is defined to be at $i=0$. The number density of the second particle at site i at time t is $n_i(t)$. Note that, since the front particle is treated separately and not included in n_i, the latter approaches the probability distribution for the second particle in the limit $\theta\to\infty$.

The only nonzero contributions to the average velocity occur when the second particle is one behind the front ($i=-1$) or on the front ($i=0$). For all other positions, the front particle undergoes an unbiased random walk, and the front does not move (on average). When $i=-1$, with proper renaming of particles, the front will move forward one step with probability 1/2, stay the same with probability 1/4, and move back one step with probability 1/4. Thus, given $i=-1$, the average velocity is $1/2-1/4=1/4$. When $i=0$, the front will move forward one step with probability 3/4 and move back one step with probability 1/4, and the average velocity is 1/2. Thus,

$$v(t)=\frac{1}{4}n_{-1}(t)+\frac{1}{2}n_0(t). \tag{4}$$

Now consider the time development. Each particle performs a random walk so that (i) if the particle is at $i=0$ at time t, $n_{-2}(t+1)=1/2$ and $n_0(t+1)=1/2$; (ii) if the particle is at $i=-1$ at time t, $n_{-1}(t+1)=3/4$ and $n_{-3}(t+1)=1/4$; (iii) otherwise, if the particle is at $i<-1$ or $i>0$, $n_{i+2}(t+1)=1/4$, $n_i(t+1)=1/2$, and $n_{i-2}(t+1)=1/4$. In these expressions the position of the second particle is defined with respect to the front at time $t+1$.

For a stationary distribution, $n_i(t)=n_i(t+1)\equiv n_i$, so the rules lead to relationships between the densities.

(a) For positions away from the front, $i<-2$ or $i>2$, we have, from (iii) above,

TABLE I. Simulation results for the velocity of front propagation and its standard deviation for low concentrations.

θ	v/θ	Std(v/θ)	Realizations	Censored steps $(40/\theta^2)$
0.0025	0.53558	0.01669	20	6400000
0.01	0.50292	0.00739	100	400000
0.05	0.50785	0.00184	1600	16000
0.1	0.50493	0.00184	1600	4000
0.2	0.49152	0.00182	1600	1000

$$n_i(t+1)=n_i(t)/2+n_{i+2}(t)/4+n_{i-2}(t)/4. \tag{5}$$

Thus, if n is stationary,

$$n_i=(n_{i-2}+n_{i+2})/2. \tag{6}$$

(b) In like manner, for positions around the front,

$$n_{-2}=n_{-4}/2+n_0, \quad n_{-1}=n_{-3}+n_1,$$

$$n_0=(n_{-2}+n_2)/2, \quad n_1=n_3/2, \quad n_2=n_4/2. \tag{7}$$

Equation (6) implies that n_i is linear in i far from the front. In order to determine the slope we need to impose boundary conditions, because we have made the approximation of only one nonfront particle, which is valid only in the region $1/\theta$ around the front. We do this by matching to the continuum solution of Eq. (3). For Eq. (3) to order θ, the density is simply θ behind the front and 0 in front of the front. Thus, to first order in concentration θ, the solution to the equations above is

$$n_i=\begin{cases}\theta, & i<0\\ \theta/2, & i=0\\ 0, & i>0.\end{cases} \tag{8}$$

Thus, from Eq. (4), $v=\theta/2$. Our simulation results, shown in Table I, confirm this prediction.

Note that, including the front particle, to first order, the stable *total* number density distribution is $N_i=\theta$ for $i<0$, $N_i=1+\theta/2$ for $i=0$, and $N_i=0$ for $i>0$. That is, we have average concentration to the left of the front and a depleted zone to the right, in agreement with simulations.

Note the bipartite nature of Eqs. (6) and (7). We can consider a simpler ''even-lattice'' model in which only the even sites are populated and still get the same average velocity. This avoids the complicating factor of a site -1 particle passing the front particle and becoming the new front particle. For the even sites,

$$n_i=(n_{i-2}+n_{i+2})/2, \quad i<-2 \quad \text{or} \quad i>2$$

$$n_{-2}=n_{-4}/2+n_0,$$

$$n_0=(n_{-2}+n_2)/2,$$

$$n_2=n_4/2. \tag{9}$$

Maintaining the same overall density θ would mean doubling the concentration at all the sites. Looking at the form of Eq. (4) and taking into account differing number densities, we get equal contributions to the velocity from site 0 and site -1, and thus the same low velocity limit $v=\theta/2$. However, this simplified even-lattice model does not approach the same limit as that of the full-lattice model at high concentration.

B. Large θ

In the full-lattice model, for any concentration the probability of the front moving backward one site is

$$P_- = \sum_{n_0=1}^{\infty} \sum_{n_{-1}=0}^{\infty} \frac{1}{2^{n_0+n_{-1}}} p(n_0,n_{-1}), \tag{10}$$

of moving forward one site is

$$P_+ = \sum_{n_0=1}^{\infty} \left(1-\frac{1}{2^{n_0}}\right) p(n_0), \tag{11}$$

and of being stationary is

$$P_0 = \sum_{n_0=1}^{\infty} \sum_{n_{-1}=0}^{\infty} \frac{1}{2^{n_0}} \left(1-\frac{1}{2^{n_{-1}}}\right) p(n_0,n_{-1}), \tag{12}$$

where $p(n_i)$ is the probability of site i having n_i particles.

With stationarity, $p(n_1(t),\ldots,n_L(t)) \equiv p(n_1,\ldots,n_L)$, we can use the dynamics of the model to obtain similar relations between the site averages and other site moments. In the rest frame of the front, if the front moves forward, site i at time t is ''fed'' by sites i and $i+2$ at time $t-1$. If the front is stationary, site i is fed by sites $i-1$ and $i+1$. If the front moves backward, site i is fed by i and $i-2$. The average at site i is

$$\langle n_i \rangle = P_+ \langle f_i + b_{i+2} | + \rangle + P_0 \langle f_{i-1} + b_{i+1} | 0 \rangle + P_- \langle f_i + b_{i-2} | - \rangle, \tag{13}$$

where f_k is the number of particles that move forward from site k, b_k is the number of particles that move backward from site k, $n_k = b_k + f_k$, $\langle \cdot | + \rangle$ means that the average is conditioned on the front moving forward, $\langle \cdot | 0 \rangle$ means the average is conditioned on the front remaining stationary, and $\langle \cdot | - \rangle$ means the average is conditioned on the front moving backward.

For example, for site $i=0$,

$$\langle n_0 \rangle = P_+ \langle f_0 + b_2 | + \rangle + P_0 \langle f_{-1} + b_1 | 0 \rangle + P_- \langle f_0 + b_{-2} | - \rangle. \tag{14}$$

Note that around the front, specifically for $i \in \{-2,-1,0,1,2\}$, the movement of the front reveals information about the number of particles at site i.

Now consider θ to be large. Assume for the moment that the distribution at all sites, including $i=0$, is Poissonian with mean θ_i, as seen in the simulations. Although this must be true far from the front, it is not clear why it is true nearby. It introduces a discrepancy of order $e^{-\theta}$ because there is a probability $e^{-\theta}$ that there will be no particles at site $i=0$. This cannot be true because $i=0$ is defined as the site of the rightmost A particle.

Neglecting this inconsistency for the moment, for large θ, one may use Eq. (14) to derive a recursion relation:

$$\theta_0 = (1-e^{-\theta_0/2}) \frac{\theta_2}{2} + \frac{\theta_0}{2} + e^{-\theta_0/2}(1-e^{-\theta_{-1}/2}) \frac{\theta_1}{2} + e^{-\theta_0/2} \frac{\theta_{-1}}{2} + e^{-(\theta_0+\theta_{-1})/2} \left(\frac{\theta_0+\theta_{-2}}{2} \right). \tag{15}$$

With the assumption $\theta_i \equiv \theta$, this equation collapses to a relation that approaches self-consistency to order $\frac{1}{2}\theta e^{-\theta/2}$.

A similar relation may be derived for the variance of the number of particles at site i,

$$\langle n_0^2 \rangle - \langle n_0 \rangle^2 = P_+ \langle (f_0+b_2)^2 | + \rangle + P_0 \langle (f_{-1}+b_1)^2 | 0 \rangle + P_- \langle (f_0+b_2)^2 | - \rangle - \langle f_0+b_2 \rangle^2. \tag{16}$$

With the Poisson assumption of mean and variance θ, this relation simplifies to an expression that is self-consistent to leading order $\frac{5}{4}\theta^2 e^{-\theta/2}$.

Using the Poisson approximation, the velocity is

$$v_P = P_+ - P_- = 1 - e^{-\theta/2} - e^{-\theta}. \tag{17}$$

We can handle $p(n_0=0)$ in another way by guessing that we should use a conditioned or truncated Poisson distribution p_T [10] because we have additional information about the probability distribution at the front, namely, we know that there is at least one particle near the front. Thus we can exclude $n_0=0$ from the Poisson approximation of the distribution. $p(n_0=0)=e^{-\theta}$ is truncated from the distribution and distributed to the other probabilities,

$$p_T(n_0=k) = \begin{cases} 0, & k=0 \\ (1-e^{-\theta})^{-1} p_P(k), & k \neq 0, \end{cases} \tag{18}$$

where $p_P(k)$ is the ordinary Poisson distribution. Then the velocity is

$$v_T = 1 - e^{-\theta/2}. \tag{19}$$

The recursion relation discrepancy for the mean is identical to that of the Poisson distribution since everything is simply divided by $1-e^{-\theta}$, and the leading order of the variance is again identical, $\frac{5}{4}\theta^2 e^{-\theta/2}$. Figure 4 shows that this agrees with the data better than Eq. (17).

This simple truncated Poisson distribution may seem promising for low concentration. It leads to the same velocity $v=\theta/2$, but it does not satisfy the recursion relations (6) and (7) to order θ. It lacks the depletion zone, so it should be regarded as only a convenient interpolation for high θ.

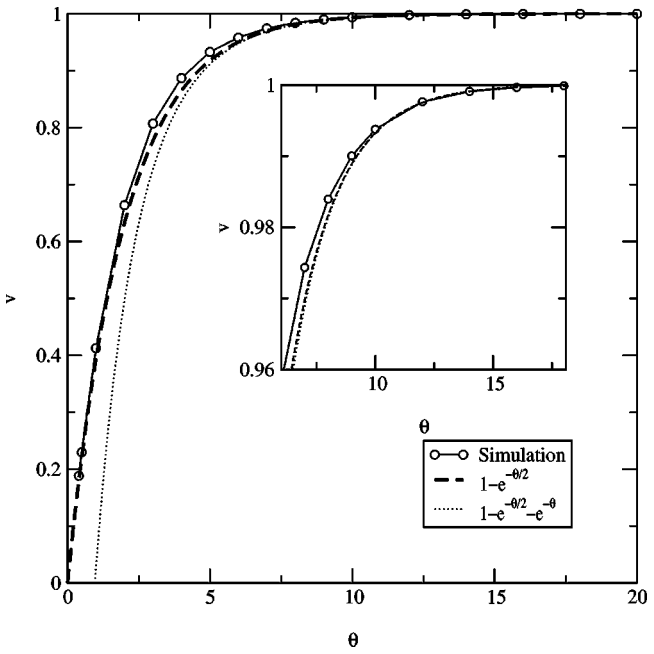

FIG. 4. Mean front velocity in lattice units/time step as a function of particle concentration.

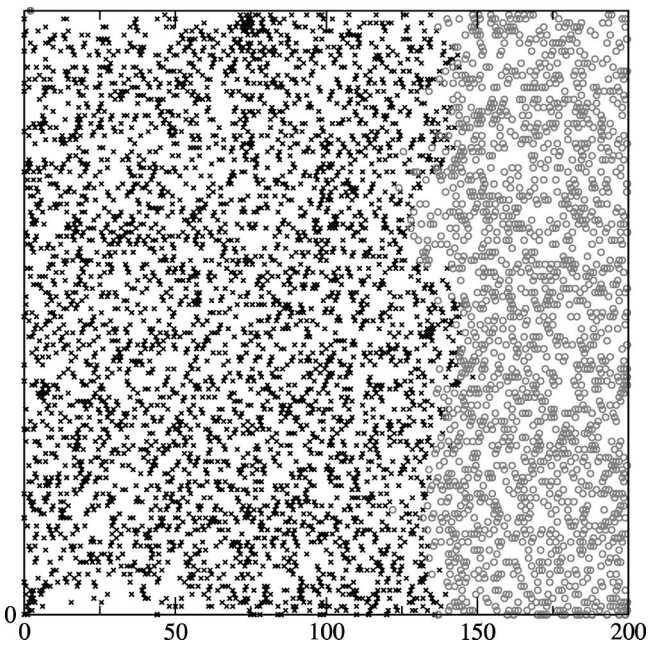

FIG. 5. Snapshot of the physical process after 2000 steps.

III. THE LOW CONCENTRATION TWO-DIMENSIONAL MODEL AND SIMULATION RESULTS

In this section, we consider a similar epidemic model in two dimensions and attempt to find out how many of the anomalous results in low concentration hold in two dimensions. For example, is the velocity smaller than the mean field result, or even linear? Is there a depletion zone in front of the front? Since we cannot generalize our one-dimensional analytic treatment, we turn to simulations.

Simulations in 2D are similar to those in 1D. However, we changed some details of the model: We used a triangular lattice in the form of a strip L sites long and M sites high with periodic boundary conditions at the top and bottom. [11]. We take the nearest neighbor distances to be 2 so that jumps from a given site (x,y) are $(x\pm 2,y)$ and $(x\pm 1,y\pm\sqrt{3})$. As above, a B particle changes to an A particle if it lands on the same site as an A particle or passes one. A typical snapshot of the process after 2000 steps is shown in Fig. 5. Note that in two dimensions a B may wander behind the front of infection and still be uninfected, although in practice this is confined to a small region near the front.

Initially, particles are randomly placed on the lattice. Those on the left half of the lattice are A's and those on the right are B's. The row front f_l is defined as the x coordinate of the rightmost A particle in row l, and the lattice front $\overline{f}$ is the average of the row fronts in the lattice. The velocity is measured as the horizontal movement of $\overline{f}$. The depletion zone is measured with respect to the front of each row and not the entire lattice.

Actually, one must be careful in making inferences from such a simulation because, with the initial Poisson distribution of particles, it can be shown that these initial conditions automatically give a depleted zone ahead of the front identical to those in the 1d case. However, we do not expect, *a priori*, that the dynamics will maintain this initial condition. Figure 6 shows that the depletion zone is, in fact, well maintained after 2000 steps with concentration $\theta=0.2$. As a check, a simulation was performed in which the bulk of the particles were randomly scattered upon the lattice as before but with two A lattice columns at the midpoint line filled solid with A particles, one A particle per site. After 2000 steps, a depletion zone again formed. In both cases there is a slight depression in the A particle concentration behind the

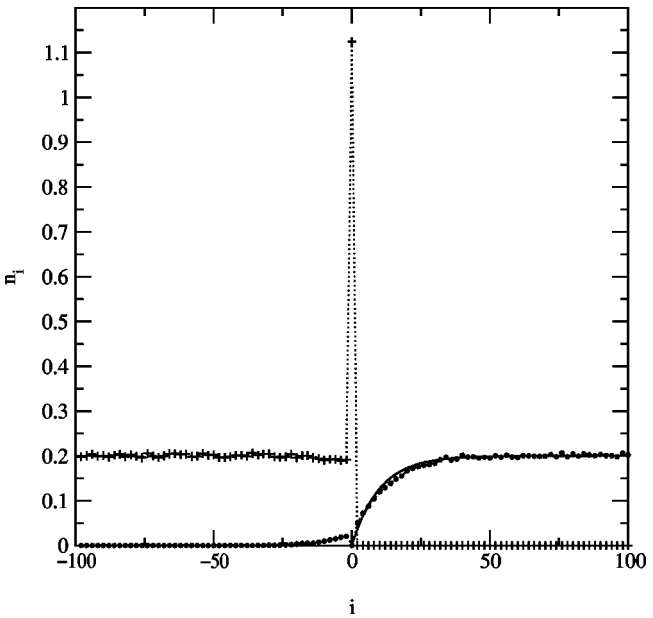

FIG. 6. Depletion zone ahead of the front after 2000 steps in 2D. Density of A (+) and (●) around the front and the exponential fit (solid line) over 200 runs.

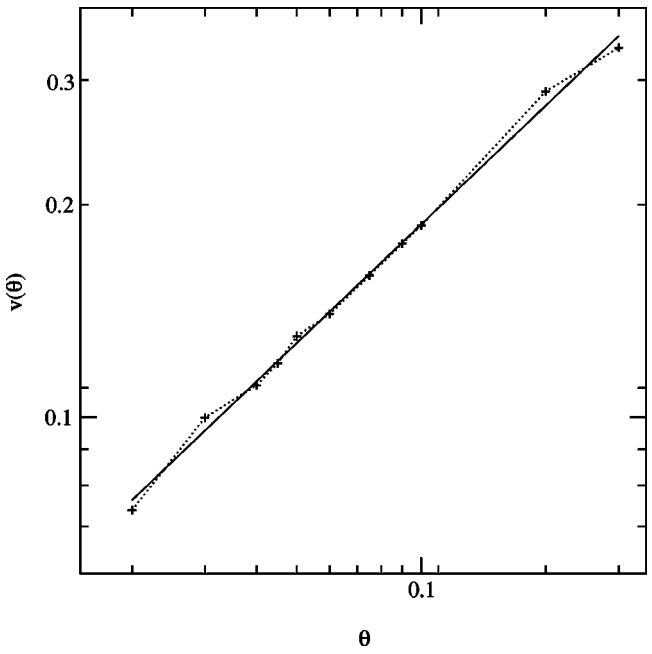

FIG. 7. Log-log plot of velocity front in lattice units/time step versus concentration in 2D. Simulation results (+) and a power law fit $v=0.079\theta^{0.559\pm0.008}$.

front as well, due to the penetration of *B* particles beyond the front.

A log-log plot of velocity versus concentration with an $L=80$ lattice is shown in Fig. 7. (We always work in the regime where the lattice width $L\gg\theta^{-1/2}$, where the scaling of the interface width might be expected; see below.) We fitted $v\sim\theta^{\gamma}$ for low concentration. Using concentrations down to $\theta=0.02$ gives an exponent of $\gamma=0.559\pm0.008$. If we include concentrations down to $\theta=0.001$, which implies an interparticle distance of ~30, the exponent increases to $\gamma=0.620\pm0.011$. Both of these results are less than the linear ($\gamma=1$) 1D result but significantly higher than the mean field exponent of $\gamma=1/2$.

In two dimensions we can investigate the front width, which is defined as the standard deviation of row fronts,

$$w(t)=\left[\frac{1}{L}\sum_{l=1}^{L}[f_l(t)-\overline{f}(t)]^2\right]^{1/2}. \tag{20}$$

When the lattice width L is much larger than the typical interparticle distance $\theta^{-1/2}$, we might expect w to satisfy the scaling hypothesis [12]

$$w(L,t)\sim L^{\alpha}f\left(\frac{t}{t_x}\right), \tag{21}$$

where $t_x=L^z$, $z=\alpha/\beta$. In the limit $t\ll t_x$ we have $w\sim t^{\beta}$, and for $t\gg t_x$ $w\sim L^{\alpha}$. This amounts to saying that the interface is self-affine [13].

For scaling, we are interested in the limit of low concentration but with the width larger than the interparticle distance, $L\gg\theta^{-1/2}$. To satisfy this condition while maintaining a manageable lattice, we chose a concentration of $\theta=0.2$, or an interparticle distance $\theta^{-1/2}\approx2.2$.

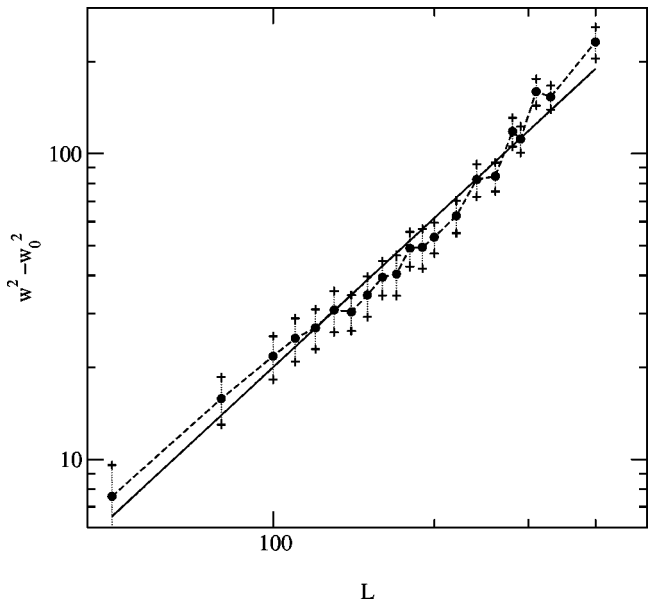

FIG. 8. Front saturation width as a function of lattice width *L*. Simulation results for $\theta=0.2$ averaged over 50 runs. Power law fit results in an exponent 2α, or $\alpha=0.84\pm0.03$.

In other chemical reaction front problems [14], the dynamics of the front are governed by the well-known Kardar-Parisi-Zhang (KPZ) equation. If the KPZ equation applies, in 1+1 dimensions the scaling exponents would be $\alpha=1/2$ and $\beta=1/3$ and thus $z=1.5$ [12,13].

In order to apply Eq. (21) we subtract off the width at $t=0$, w_0. We plot $w^2-w_0^2$ versus t and look for scaling as

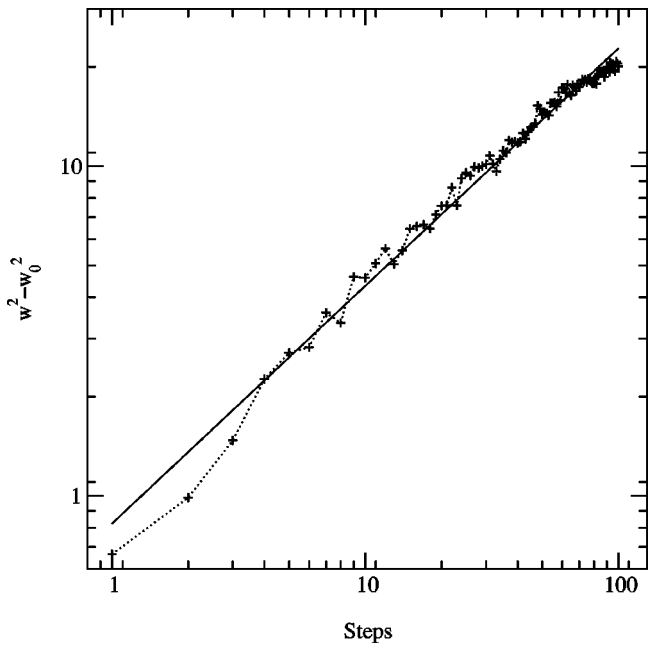

FIG. 9. The front width as a function of time. Simulation results for $\theta=0.2$ averaged over 200 runs. Power law fit results in an exponent $\beta=0.344\pm0.004$.

described above. As shown in Figs. 8 and 9, we measure $\alpha=0.84\pm0.03$ and $\beta=0.344\pm0.004$, which implies $z=2.4$. In an independent analysis, we tried to rescale the data for $\theta=0.2$ and varying widths and collapse them onto one line. Crossover times $t_x=L^z$ were judged by eye, and they were difficult to judge precisely. However, this independent analysis yielded $z=2.6$. Others have found that similar models do not satisfy the KPZ equation. In their analysis of $A+A\leftrightarrow A$, Riordan, Doering, and ben-Avraham [5] calculated the interface width to satisfy the scaling hypothesis with exponents $\alpha=0.272$ and $\beta=1.00$ [15]. In fact, Tripathy and van Saarloos [16] have shown that, even if the FK equation were obeyed by this model, we would not expect KPZ scaling.

This analysis assumes that the front is self-affine. However our value of $\alpha\approx1$ is consistent with a self-similar front. Further work will be necessary to resolve this question.

IV. SUMMARY AND DISCUSSION

We have shown that in low concentration the dynamics of $A+B\rightarrow2B$ are significantly different from what would be expected from mean field theory, even in 2D. We have seen that in 1D the behavior of v at low concentration can be traced to the depletion zone to the right of the front. Near the front the distribution of particles is very different from the Poisson distribution, and the motion of the front is dominated by the depletion. In the low concentration limit, to order θ, the velocity is simply $v=\theta/2$. For large θ, the velocity is approximated by $1-e^{-\theta/2}$, and the distribution is quite close to the truncated Poisson distribution.

In 2D, we also find a depletion zone, and $v\sim\theta^{0.6}$, significantly different from the mean field result. If we assume that the front is self-affine, we measure scaling exponents of $\alpha=0.84\pm0.03$ and $\beta=0.344\pm0.004$, significantly different from the KPZ model.

These results have applications to the spatial distribution of real epidemics and chemical reactions. How different the results are from the mean field continuum model depends upon the dimensionality of the underlying structure or the underlying spread. The smaller the dimension, the more important the fluctuation effects. Epidemics have often been modeled to occur on a percolation cluster. In such a disordered 2D medium, we would expect the dynamics to be governed by bottleneck effects and thus more similar to the 1D result.

ACKNOWLEDGMENTS

We are grateful to Martin Barlow and Igor Sokolov for useful discussions. This work is supported by DOE Grant No. DEFG-02-95ER-45546.

[1] J. Mai, I. M. Sokolov, and A. Blumen, Phys. Rev. Lett. **77**, 4462 (1996).
[2] J. Mai, I. M. Sokolov, and A. Blumen, Europhys. Lett. **44**, 7 (1998).
[3] E. Brunet and B. Derrida, Phys. Rev. E **56**, 2597 (1997).
[4] D. A. Kessler, Z. Ner, and L. M. Sander, Phys. Rev. E **58**, 107 (1998).
[5] J. Riordan, C. Doering, and D. ben-Avraham, Phys. Rev. Lett. **75**, 565 (1995). These authors model the reversible version of this reaction, $A+B\leftrightarrow2A$, by looking at $A\leftrightarrow2A$. This model differs from ours in that B is assumed to be in excess or otherwise maintained at a steady level. They thus suppress any variation in B, and this spatial variation in B is at the heart of our analysis and results, as we will see.
[6] R. A. Fisher, Annals of Eugenics **7**, 355 (1937); A. Kolmogorov, I. Petrovsky, and N. Piscounov, Moscow Univ. Bull. Math. **A1**, 1 (1937).
[7] J. D. Murray, *Mathematical Biology* (Springer, Berlin, 1993).
[8] We used a version of periodic boundary conditions appropriate to this problem: A's that walked off the left edge were added to the right edge as B's and vice versa.
[9] A preliminary version of these results was presented in C. Warren, E. Somfai, and L. Sander, Braz. J. Phys. **30**, 157 (2000).
[10] V. K. Rohatgi, *An Introduction to Probability Theory and Mathematical Statistics* (Wiley, New York, 1976).
[11] In 2D, we used periodic boundary conditions on the top and bottom of the strip, and the same conditions on the ends of the strip as in 1D.
[12] M. Plischke and Z. Racz, Phys. Rev. A **32**, 3825 (1985); F. Family, and T. Vicsek, J. Phys. A **18**, L75 (1985).
[13] A. L. Barabasi and H. E. Stanley, *Fractal Concepts in Surface Growth* (Cambridge University Press, New York, 1995).
[14] R. Goodman, D. Graff, L. M. Sander, P. Leroux-Hugon, and E. Clement, Phys. Rev. E **52**, 5904 (1995); L. M. Sander and S. V. Ghaisas, Physica A **233**, 629 (1996).
[15] However, Riordan *et al.* [5] use an ensemble average in their definition of interface width, where we use a lattice average.
[16] G. Tripathy and W. van Saarloos, Phys. Rev. Lett. **85**, 3556 (2000).